

<sup>1</sup> Дипломна робота  
<sup>2</sup> Supervisor(CERN): Massimiliano Ferro-Luzzi

<sup>3</sup> Bereziuk Ivan  
<sup>4</sup> 27 травня 2015 р.

## 5    1 STRAW tubes

6    The option for STRAW tubes is similar as in NA62 experiment with one main  
7    difference – the length is twice longer( 5m versus 2.1m).

8    The next table. 1 describe STRAW tube options.

Parameter name	Value
wire	$30\mu m$ gold-plated Tungsten
straw length	5m
Voltage	1750V
inner tube radius	9.8 mm
wire medium density	$19.3 \text{ g/cm}^3$
Wire tension	$\sim 90 \text{ g}$
Working tube gas mixture	Ar70% CO <sub>2</sub> 30%

Табл. 1: STRAW tube parameters

## 9    2 Signal

10 Computer program Garfield [1] is designed for detailed simulation of two- and  
11 three-dimensional drift chambers. So we will perform STRAW tube studies using  
12 this program.

13    Charged particle create elector-ion pairs wile traverse the drift tube. Electrons  
14 under affecting the electric field drift to the wire anode 1. During the travel they  
15 increase their energy and invoke avalanche. Therefore they produce a measurable  
16 signal.

17    Initial electrons drift to the wire due to the electrical field between the wire  
18 and the tube wall. Electrons ionize gas molecules due to the high electric field  
19 around the wire, especially near the wire when the electric becomes very strong.  
20 Subsequently readout electronics process the signal induced on the wire.

21    The event registers if signal reach some a threshold voltage (Fig. 2). So the  
22 value of threshold is a key factor on the way of searching optimal setting for  
23 signal processing procedure.

24    We have to set threshold as low as possible but enough far from noise to  
25 achieve highest value of relation true/false detected track and tube efficiency.

26    A variation of the signal height introduces a variation in the time when the  
27 signal passes the threshold and is considered to be the main contribution to the  
28 STRAW tracker resolution.

29    In the track reconstruction software(GARFIELD [1] an effective TR-relation  
30 is used. It only describes the relation between the drift time and the distance  
31 from the track to the wire, which differs from the distance to the ionization  
32 cluster. The shape of the TR-relation is defined by the drift velocity of the  
33 ionization cluster inside the straw. The electric field increases towards the wire,

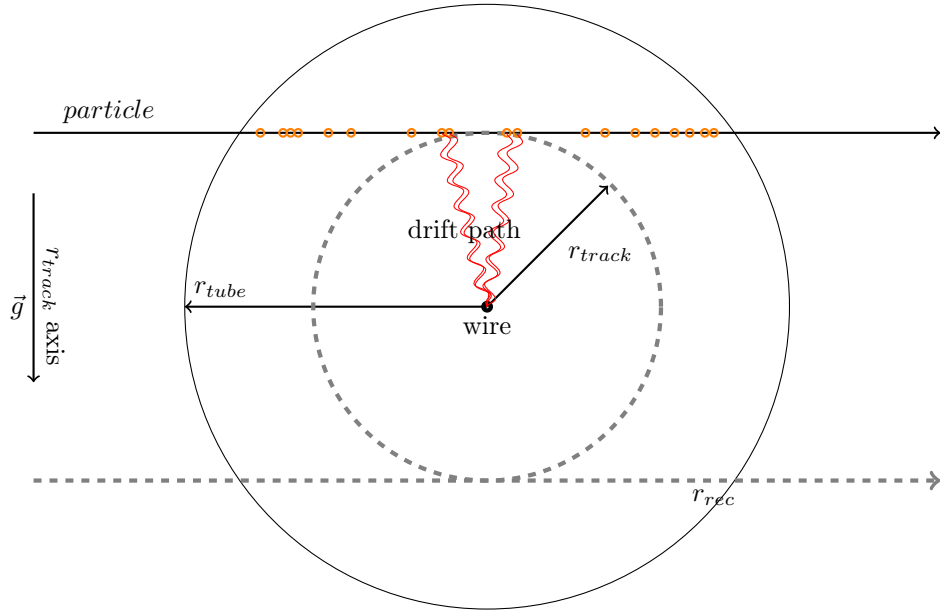


Рис. 1: Schematic view of a particle passing the straw and producing ionization clusters. The ionization cluster electrons drift to the wire and induce the signal. Only the earliest signal is detected. The closest distance from the track to the wire,  $r_{track}$ , and radius of the straw,  $r_{tube} = 2.45\text{mm}$ , are also indicated.

<sup>34</sup> leading to a non linear TR-relation. Currently almost parabolic dependence is  
<sup>35</sup> used, and easily can be fitted by function (??).

<sup>36</sup> The drift time versus the unbiased distance distribution and the result of the  
<sup>37</sup> fit are shown in Fig. 13a. Noise hits under the main distribution, i.e. at earlier  
<sup>38</sup> times, are due to primary or secondary particles ( $\delta$ -rays) passing the straw at a  
<sup>39</sup> closer distance to the wire, consequently producing an earlier signal.

<sup>40</sup> Muon  $\mu$  was chosen as test particle for simulation with energy 1GeV. You  
<sup>41</sup> can see some of typical tracks from the  $\mu$  through the tube Fig.7a,7b. Initial  
<sup>42</sup> clusters along the track are marked by orange points on the figure.

### <sup>43</sup> 2.1 Leakage noise

<sup>44</sup> Every time we deal with different kind of noise. Basically it is noise from leakage  
<sup>45</sup> current through readout electronics.

<sup>46</sup> As will be discussed further we analyse not the current invoked by particle  
<sup>47</sup> but the output voltage from amplifier. In GARFIELD we able convolute input  
<sup>48</sup> current  $I(t)$  with electronic response function (1):

$$f_{resp} = A \cdot (e^{-t/0.005} - e^{-t/0.030}) \quad (1)$$

<sup>49</sup> Noise is very important for every calculations and it makes bit impact on

50 straw precision and straw efficiency. So we can't rely on results until we receive  
 51 signal and noise from real STRAW tube prototypes.

52 Convolution smooth input current. Experiments that used to drift tubes  
 53 (such as ??(advise of Iouri Guz)) say that the noise should have gauss distri-  
 54 bution with RMS equal to a amplitude of signal from 2000 electron in the tube -  
 55 electric noise charge (ENC). (**This part should be clarified more precisely. Would**  
**be good to include some results from noise measurements from STRAW tube**  
**samples.** In fig.2 you can see deposition from noise marked by blue line.

56 On the figure fig.2 The time stamp  $Time = 0$  correspond to the time muon  
 57 cross tube. The convolution function smooths and spreads input current. It  
 58 mean that the output voltage in GARFIELD does not contain part of signal  
 59 before hit event time stamp.

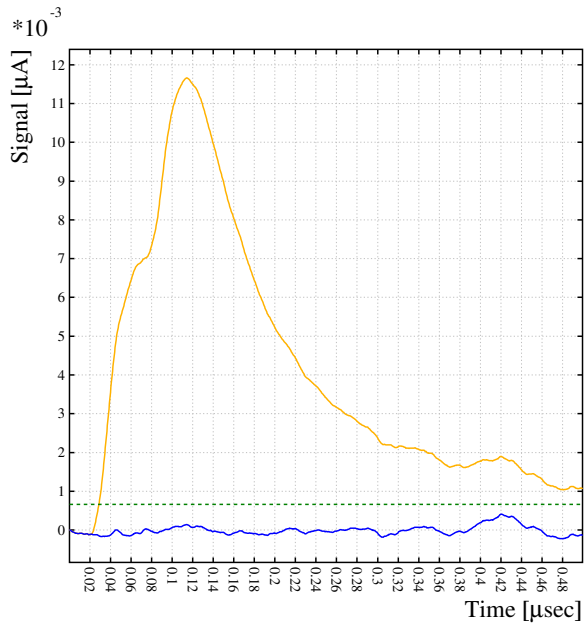


Рис. 2: Example of output signal  $V(t)$  after convolution(front-end electronics) from central track(yellow line). The noise component of the same signal depicted by separate blue line. Grin dashed line is a threshold for trigering drift time and equal to  $5\sigma$  of noise distribution.

## 62 2.2 STRAW efficiency

63 The interaction of charge particle with gas molecules nave probabilistic nature.  
 64 For short distance tracks(somewhere at the tube periphery) the probability of  
 65 tracks that do not produce any electron/ion pair becomes significantly high.

66 The number of produced ionization clusters directly affects the hit efficiency  
 67 profile. [2] Smaller ionization length increase hit efficiency because of more  
 68 ionization clusters per length unit are producing. In GARFIELD we can easily  
 69 calculate amount of clusters per track. In fig. 4b you can see a distribution of  
 70 number of clusters per central track for our STRAW tube. It mean that straw  
 71 efficiency will be lower at the tube wall( see fig. ??).

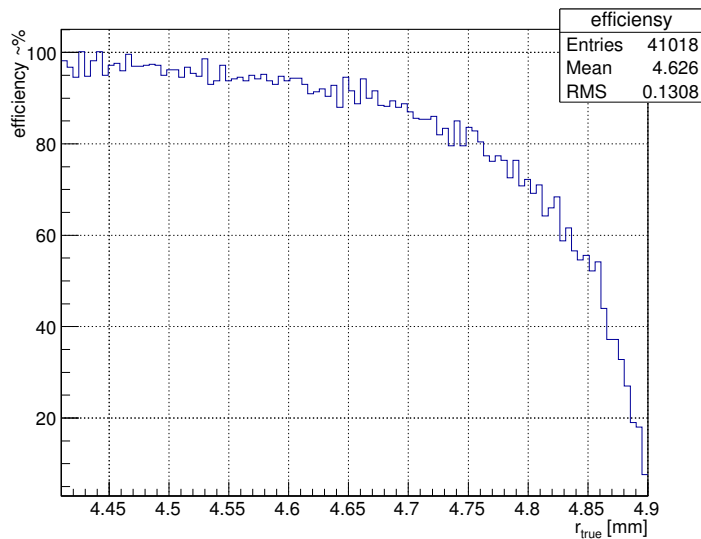


Рис. 3: Straw tube efficiency. Result of homogeneous penetrating periphery of tube by 50k events(scaled down by factor of 5.  $\frac{50k \text{ events}}{100\text{bin}} = 500 \frac{\text{eventst}}{\text{bin}}$ ).

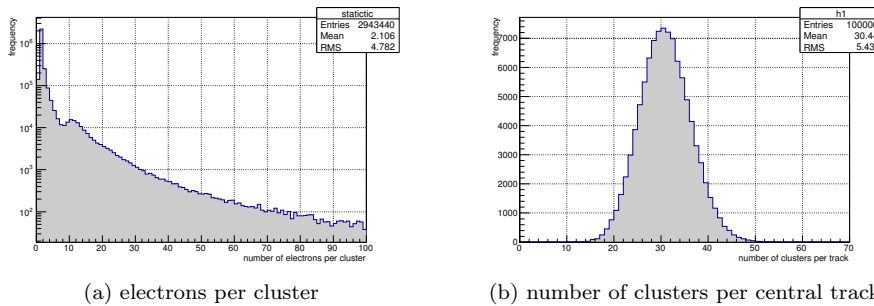


Рис. 4: There are big amount of graphs. So I'm trying to pair it. ere we can write something if needed. Some common description of (a) and (b) figures?

72 From the figure ?? we can conclude that the efficiency of tube is 100% almost  
 73 in whole region covered by tube except pre wall region which is quite small.

<sup>74</sup> Increasing the gas mixture density or increasing the tube radius for the same  
<sup>75</sup> gas density can increase tube efficiency. Have to check this in feature studies.

### <sup>76</sup> 3 Gain

<sup>77</sup> If multiplication occurs, the increase of the number of electrons per path  $ds$  is  
<sup>78</sup> given by

$$dN = N\alpha ds \quad (2)$$

<sup>79</sup> The coefficient  $\alpha$  is determined by the excitation and ionization cross sections  
<sup>80</sup> of the electrons that have acquired sufficient energy in the field. It also depends  
<sup>81</sup> on the various transfer mechanism and electric field  $E$  and increases with the  
<sup>82</sup> field because the ionization cross-section goes up from threshold as the collision  
<sup>83</sup> energy  $\varepsilon$  increases. As we can suppose the coefficient  $\alpha$  is of big amount of  
<sup>84</sup> parameters.

<sup>85</sup> The amplification factor  $G$  on a wire(that is more interesting for us) is given  
<sup>86</sup> by integrating (2) between the point  $s_{min}$  where the field is just sufficient to  
<sup>87</sup> start the avalanche and the wire radius  $a$ :

$$G = N/N_0 = \exp \int_{s_{min}}^a \alpha(s) ds \quad (3)$$

<sup>88</sup> GARFIELD can provide us by amplification factor  $G$  for any point of the  
<sup>89</sup> tube(because  $G$  is coordinate dependent magnitude). The amplification factor  
<sup>90</sup> is equal almost in whole tube space except neighbourhood near the wire because  
<sup>91</sup> electric field becomes significantly high only near the wire (see figs 5a, 5b). When  
<sup>92</sup> the wire is shifted from the center of the cube the electric field in area close to  
<sup>93</sup> the wire is the same as in centered state. So the amplification factor  $G$  is quite  
<sup>94</sup> similar in both cases.

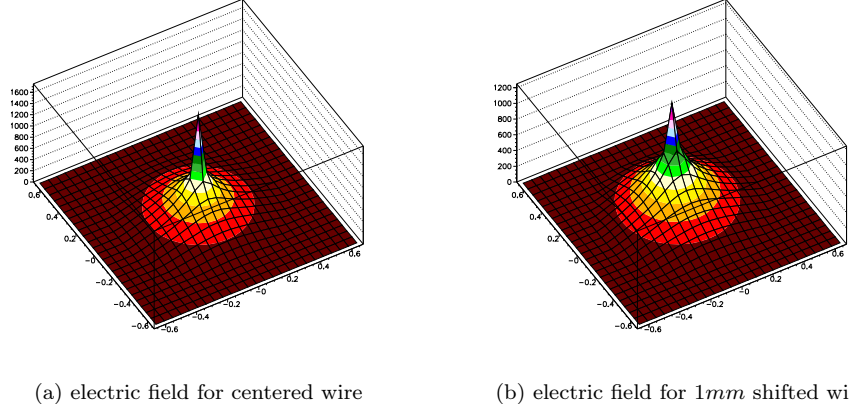
<sup>95</sup> Implementation of gain value calculation is not so reliable in GARFIELD(especially  
<sup>96</sup> fortran version). So we can reach better results using Garfield++ (which is newer  
<sup>97</sup> and take into consideration more effects).

<sup>98</sup> On the Fig. ?? you can see that the gain  $G(V)$  have precisely exponential  
<sup>99</sup> dependence. This is frankly does not inspire confidence. The difference can be  
<sup>100</sup> up to 100% (as Rob Veenhof - creator of GARFIELD [1] said).

### <sup>101</sup> 4 Wire sagging

<sup>102</sup> Easy to predict that the displacement of the wire invokes distorting an electric  
<sup>103</sup> field(see figs 5a,5b) and drift path for electrons/ions inside the tube(see fig.7a  
<sup>104</sup> and fig.7b). The rt-relation for track reconstruction directly depend on the wire  
<sup>105</sup> position in the tube. So rt-relation lose it's previous symmetry(see next sections).

<sup>106</sup> The direction of sagging is unpredictable when the wire is centered and the  
<sup>107</sup> straw has vertical orientation. Impact of gravitation field into the wire does



(a) electric field for centered wire

(b) electric field for 1mm shifted wire

Рис. 5: Electric field intensity map for different wire position in the cube calculated in GARFIELD software. Conditions for those plots are described in table 1

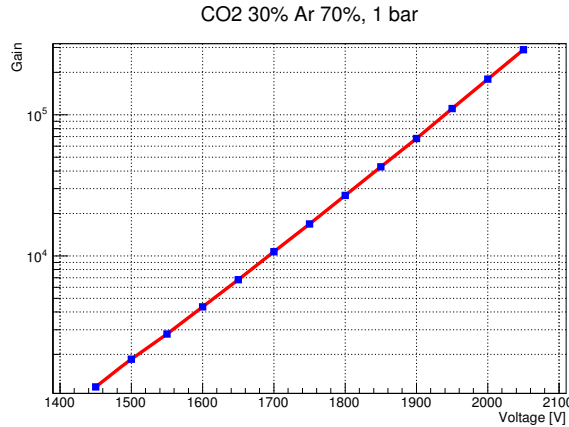


Рис. 6: Dependence of the gain of the voltage applied to the wire. The rest of STRAW tube settings you can find in table 1. [need add gain\(v\) graph for shift wire STRAW tube for comparison](#)

not make any effect in this state. But we can avoid this ambiguity by setting straws horizontally. This condition is necessary to make track reconstruction possible. Even when strung with a pulling force  $T$  close to the breaking limit, wires in several metre long tubes will experience a gravitational sag that is large in comparison with the achievable accuracy of drift tubes.

We estimate significant wire sagging(by comparison to the tube radius) because of wire attracts to the tube under affecting of gravitation and electric

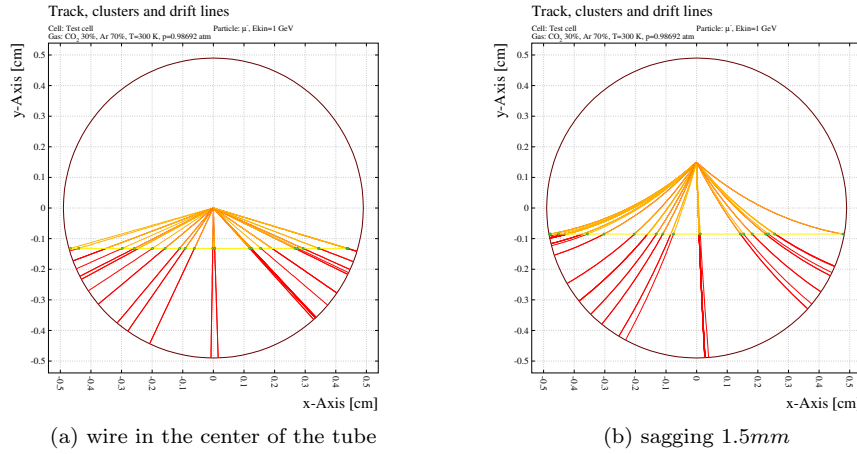


Рис. 7: An example of tracks from the on the tube for different position of the wire from GARFIELD simulations. Initial clusters marker by green. Drift lines for electrons marked by yellow, ions – red lines.

<sup>115</sup> field force.

<sup>116</sup> You can see a profile of wire sagging of 5m length wire in 1cm diameter  
<sup>117</sup> straw tube and 1750V voltage on the fig.8 calculated in GARFIELD software  
<sup>118</sup> [1].

sag profile for 5m long straw

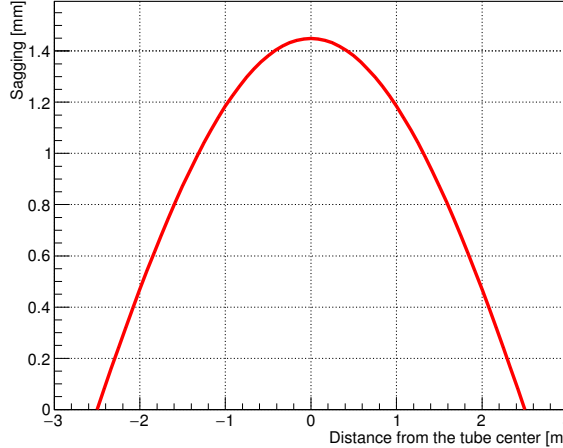


Рис. 8: Wire sag profile under electric and gravitation field calculated in GARFIELD. All options for this straw system are described in table 1.

<sup>119</sup> The calibration of STRAW tube with sagged wire is more difficult by compari-

120 son to the mode without sagging.

121 Variation of wire tension, wire radius should be taken into account as high  
122 affect factor for sag value.

## 123 5 Sag estimation

124 In this section we have to find out method for assessing sagging. This is key  
125 step that makes track reconstruction procedure possible.

126 At first we have to think on data we can use for such kind of calculations.  
127 Much attractable information we can extract from drift time distribution.

128 The wire sags under electric and gravitation force. Therefore the sag value  
129 is differ along the tube(fig 8). But we can separate collected data for different  
130 position along the tube. STRAW tube detector consist of several parallel layers  
131 of tubes at some angle to each other. So we can easily fix longitudinal position for  
132 tracks that cross several crossed tubes(at least two). Collimation is also possible  
133 via scintillator triggering before and after STRAW tube.

134 Lets say we can install our STRAW tube into homogeneous particle flow and  
135 save drift time distribution for some narrow section of the tube. These distri-  
136 butions are different from each other(see example on Figure ??). The difference  
137 between diagrams increasing with sag difference. So it is good possibility for sag  
138 calibration.

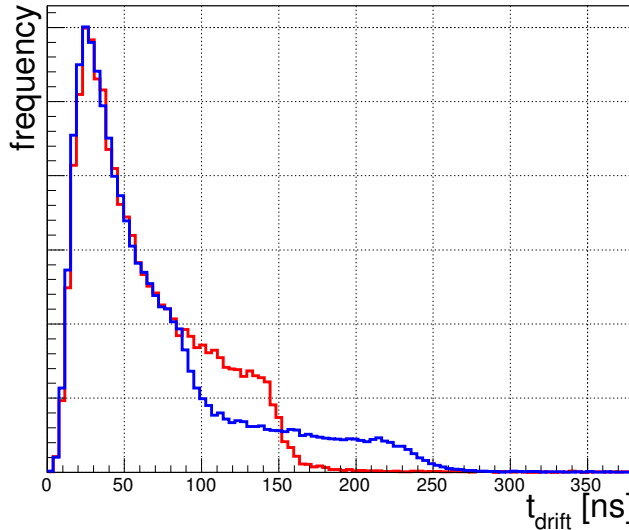


Рис. 9: Drift time distribution for a homogeneous irradiation with a centered wire (red) and for a wire offset of 0.9 mm (blue).

139 Then we have to bind each drift time distribution with appropriate sag value.

**140** This is part of laboratory work when sag profile measurements can be performed  
**141** via optical method prior to the exposition.

**142** Distributions on graph ?? contain GARFIELD simulations for some certain  
**143** wire(not for section of sagged wire)because of GARFIELD can handle only two-  
**144** dimensional tasks.

**145** Lets say we have an equipment for scanning the tube to measure wire sagg-  
**146** ing profile. After profile measurements we divide our tube into sections. Wire  
**147** position within separate section should be within desired precision.

**148** So we need divide our tube into 57 sections (see figure 10) if maximum of  
**149** wire offset(at the center of the tube) is equal to  $1.45mm$  and desired precision  
**150** is  $50\mu m$ .

$$N_{halftube} = \frac{1.45mm}{50\mu m} = 29; \quad (4)$$

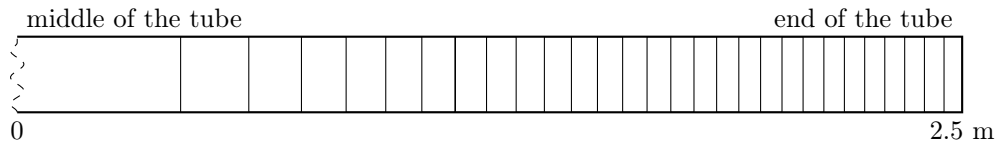


Рис. 10: Tube sectioning. Sag value at the tube center is  $1.45mm$ . Difference of wire sag value from section to section is  $50\mu m$

**151** Then we need an exposition of sufficient number of events for every of secti-  
**152** ons(at least 50k events). There can be troubles time of exposition time because  
**153** square of sections at the end of the tube is quite small. So the time of exposition  
**154** of distant sections will be inversely much longer.

**155** The next step is to find dependence of dt-distribution shape with wire offset.  
**156** The point that we can evaluate matching between histograms via  $\chi^2$  criteria.  
**157** As we can see in the figure 11a the comparison of  $\chi^2$  has smooth dependence  
**158** across increasing of wire offset for high statistic histograms.

**159** First steps for sag estimation are:

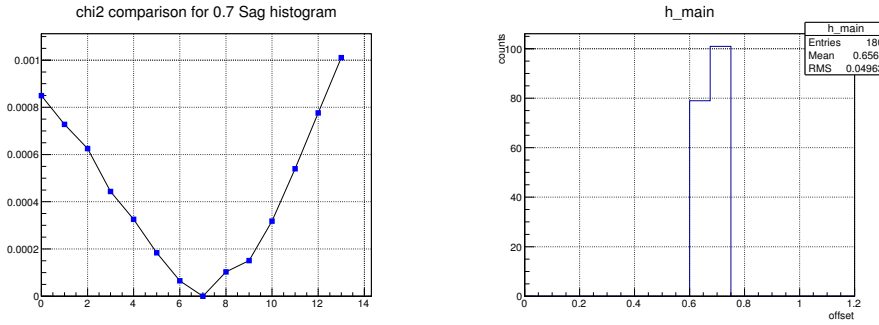
- 160** 1. measure wire sag profile via optical method;
- 161** 2. make a sectioning for wire sag profile;
- 162** 3. collect enough amount of events for every of dt-distribution and save this  
**163** core distribution for further comparisons.
- 164** 4. measure dt-distribution for new drift tube section that is subject of study.
- 165** 5. calculate  $\chi^2$  criteria for this current dt-distribution with each of core di-  
**166** stribution.

167    **5.1 Finding most probable value of wire displacement for  
168    certain point of the tube**

169    **5.2 Raw method**

170    The simplest method to find  $S$  is to equate it to the corresponding value of best  
171    matched core DT-histogram.

172    On the figure 12b you can see distribution of such kind of reconstruction.  
173    Even for 5k events td-distribution in this case the precision can be quite high( $\sim$   
174     $50\mu m$ ).



(a) Series of  $\chi^2$  of comparison  $0.7mm$  sag core td-distribution with each each of core histograms. 14 core histograms for sag dipason  $0 \dots 1.3mm$  with step of  $100\mu m$

(b) Distribution of wire offset reconstruction from 180 series 5k events each. 50k events for core template histograms. True bias is  $0.63mm$ . 1 bin =  $0.1 mm$ .

Рис. 11: Wire position(displacement) reconstruction

175    **5.3 "Minimum of  $\chi^2$  as linear approximation"**

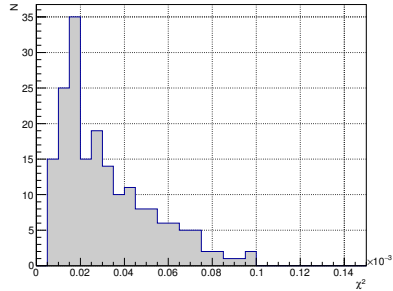
176    But what is most probable value of wire displacement  $S$  in this case? Probably  
177    somewhere between them. So can we go in more clever way to reach better  
178    result? Probably yes.

179    If dependence of  $\chi^2$  criteria of wire displacement  $S$  for near to the true  
180    position region is linear(that certainly is not a true, but as first approximation)  
181    than we can easily find this intermediate value of wire displacement.

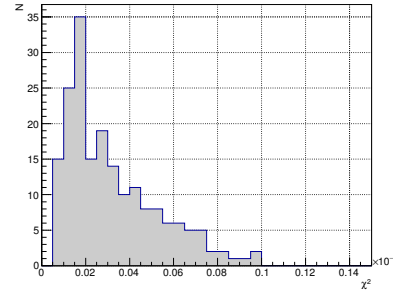
182    There we proceed in two steps. The first is raw estimation of wire dis-  
183    placement as in above mentioned method.

184    For the second step we need to know some additional estimations. The first  
185    question is how small can be  $\chi^2$  it our case? Lets fix statistic on 50k events  
186    for one DT-distribution. This value should a bit depend for different  $S$ . But  
187    for now lets consider that it is a constant value. From the figure 12a you can  
188    see distribution of  $\chi^2$  from comparison of 20 DT-distribution<sup>1</sup> for  $S = 0.7mm$ .  
189    Mean value + RMS of distribution is  $5.3 * 10^{-5}$ . So if some of the  $\chi^2$  is higher  
190    than this threshold than we go for second stage.

<sup>1</sup> pair comparison give us  $C_{20}^2 = \frac{20!}{2^{10}18!} = 190$  different combinations



(a)  $\chi^2$  distribution of comparison of 20 DT-distributions diagrams each other ( $C_{20}^2 = 190$  combinations)



(b)  $\chi^2$  distribution of comparison DT-distribution histograms 0.7mm S vs 0.8mm here I estimate much narrow distribution. Image to be inserted

Рис. 12:  $\chi^2$  distributions.

191 On the figure 12b you can see distribution wire sag calculation for 180 histograms  
 192 with 5k events statistic. Precision in this case  $\sim 50\mu$ . The algorithm  
 193 of sag estimation is pretty simple: wire offset value equal to the best match  
 194 between *test* and *core* histogram.

195 After we know sag value at some points of the tube or every where we can  
 196 make one awesome collective analysis. The smoothing of wire offset value along  
 197 the tube will give us much more precision results. Fitting of sag value at every  
 198 point of  $s(l)$  by some parabolic function should provide us the best results.

#### 199 5.4 Wire sagging profile finding

200 to be completed ...

201 Here i would like to put total plot of wire sag profile and compare reconstructed  
 202 profile with true profile.

#### 203 5.5 Practical measurements of DT-distribution

204 We need second detector that can measure position of muon that hit STRAW  
 205 tube. It can be Si strip(or pixel) sensor based detector or detector based on  
 206 scintillation with the same destination.

207 Each kind of detector have it's own advantages and disadvantages. The  
 208 potential cell unit (strip or pixel) of Si detector will be smaller than in scin-  
 209 tilator but also is much expensive. At the current stage we deal with 1cm  
 210 diameter tubes. So scintillator is primal target. But it can shift to the Si sensors  
 211 if scintillators will not provide satisfied precision.

212 Preliminary chem of DT-measurements you can see on the picture fig ??

## 213 6 Track reconstruction

214 The time between the track hit time stamp and the signal rising edge is a  
 215 measure of *drift time* of these electrons. The relation between the *drift time*  
 216 and the distance from the track to the center of the tube(wire while no sag for  
 217 centered wire) is called *drift time - distance relation* or *tr-relation*.

218 The drift time  $t$  is a function of track position relative to the wire(so it's  
 219 means the track position) and electric field along the drift trajectory.

220 Assumed that the working position for straws will be parallel to the particle  
 221 bunch, and acceptance of particle spreading will not be significantly big. So  
 222 tracks will be collinear each other within every separate STRAW tube unit.

223 Summing the above mentioned we have one dimension task – reconstruct  
 224 tracks on vertical axis<sup>2</sup> (see examples of outcome tr-distribution  $t = t(r, s = 0)$   
 225 in Fig.13a and Fig.13b) even the wire sagging. Sagging will be always down  
 226 thanks to gravitation force  $\vec{g}$ .

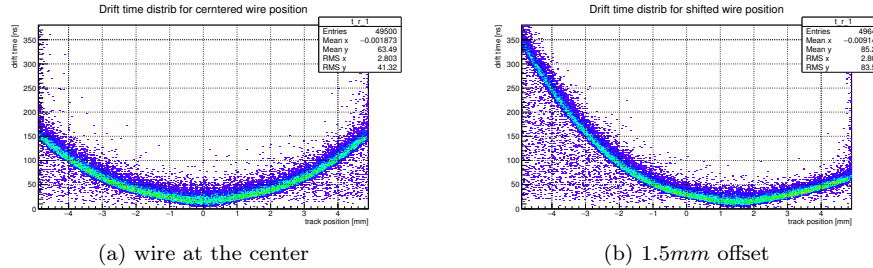


Рис. 13: Distribution of drift time  $t_{drift}$  as function of track position  $r_{track}$  relatively to the tube center

227 The rt-relation is differ along the tube because different wire position  $s$ . Thus  
 228 we have for the drift time

$$t_{drift} = t_{drift}(r_{track}, s) \quad (5)$$

229 The idea to STRAW tube is to find the inverse dependence

$$r_{track} = r_{track}(t_{drift}, s) \quad (6)$$

230 From the section "Sag estimation"we can find sag profile for straw. Therefore  
 231 the rt-calibration becomes 1 dimension less:

$$r = r(t, s = const) \quad (7)$$

### 232 6.1 How drift time resolution depend on wire offset?

233 Distorting of electric field inside the tube invoked by wire displacement from the  
 234 center position will make an effect on drift time. Here we are going to estimate  
 235 magnitude of drift time change.

<sup>2</sup>An example of single track reconstruction which explains the approximate procedure of reconstruction you can see on Fig.1

236 As was noted above we make a binning for our data along the  $r_{track}$  (fig. 13a,  
237 13b). The resolution at every bin is RMS of every bit digram (fig.??).

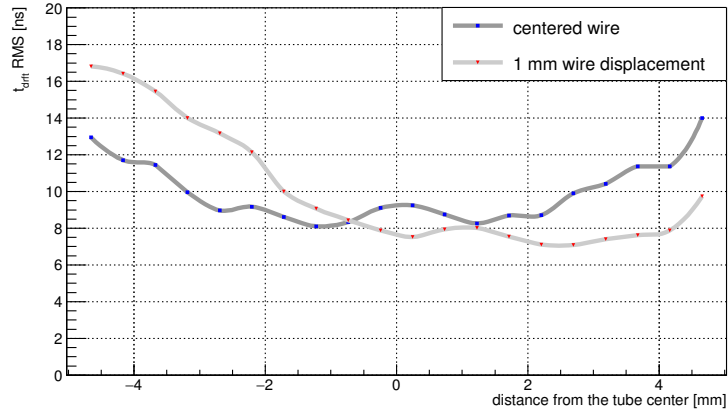


Рис. 14: Resolution of drift time as a function of distance from the wire.

238 We are dealing with probabilistic nature of clustering that spread rt-relation  
239 from thin line. The leakage noise is also present in calculation but the effect of  
240 it is not very high (especially in this calculation).

241 Every plot of output current (see fig. 2) consist of 1000 equidistant frames.  
242 The threshold is set to  $5\sigma$  of noise. Leakage noise make effect on drift time  
243 measurements in case its amplitude becomes higher than threshold value in  
244 range from  $t = 0$  to  $t = t_{drift}$ . At five-sigma there is only one chance in nearly  
245 two million that a random fluctuation would yield the result. The drift time for  
246 tracks close to the tube edge can be up to 150 ns and 300 ns in case wire displaced.  
247 The probability to meet noise above threshold value is less than 0.02%.

248 Another source of noise points on tr-distribution comes from  $\delta$ -electrons that  
249 cause secondary ionisation in tube volume. The impact do only those electrons  
250 which are emitted in the direction of the wire (see example on fig. 15a).

251 The number of events out of TR-ralation because of  $\delta$ -electrons is quite small.  
252 Especially percentage of events where  $\delta$ -electrons make effect on drift time is  
253 less than 1% of total number of events in GARFIELD simulations.

254 Tube wall is very thin but particle still can cause  $\delta$ -electrons when crossing  
255 it. GEANT4 studies show that such kind effect also presents in interaction of  
256 muon with tube volume, and percentage of events with  $\delta$ -electron that affect  
257 drift time even less than 0.2%.

## 258 6.2 Finding of rt-relation

259 The rt-relation depict relation between drift time and track position. The idea is  
260 to find the best fit of give data to achieve higher resolution and avoid systematic  
261 errors.

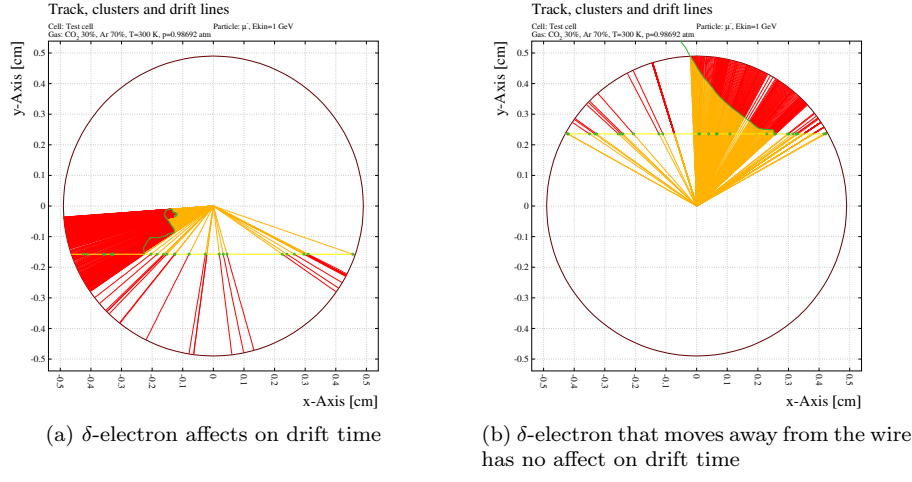


Рис. 15: Garfield simulation with  $\delta$ -electron presence. Red lines - ion trajectory, yellow - electrons. Trajectory of  $\delta$ -electron marked by green curve line.

262     The problem that we have to minimize influence of noise while fit. One  
 263 suppose that the noise have approximately homogeneous distribution of points  
 264 that locates below the main line of distribution. Consequently we can filter it  
 265 by fitting only points from regions with local point density higher than some  
 266 threshold value. Another way is to make a binning our distribution along the  
 267 track position and fit every 1-D histogram by Gaussian. The fit points of Gaussian  
 268 mean values by fit function.

269     Nevertheless our data contain very small amount of "non-track" points.

270     TR-relation is asymmetry relatively to the  $r = 0$  almost in all cases except  
 271 wire in the center of the tube. Therefore we have to calibrate for every of  
 272 branches. It means we need to find two track positions for every of drift ti-  
 273 me value and reject one of them in further data processing stages.

274     In previous section we found way to measure wire sag profile. So we can  
 275 use this trick in present stage for separating data into "right" and "left" branch.  
 276 Every of branches we will calibrate separately.

277     Lets suppose we can fit every of tr-diagram by pair of analytic fit function  
 278 (8):

$$t(r_{track}) = e^{a_0 + a_1 r_{track}} \quad (8)$$

279     If the figure ?? you can see tr-relation. Fitting is not perfect because of using  
 280 simple fit function template (8). But we will use reverse to the (8) relation,  
 281 because we have to find  $r_{track}$  from known  $t_{drift}$ . We can do it be because the  
 282 aim of this studies is not a precision calibration but global evaluation affect of  
 283 wire sagging into total result.

284     As you can see in the figure ?? red fit line does not cover whole drift time  
 285 spectre. So events with drift time less than covered range(less than  $\sim 20ns$ )

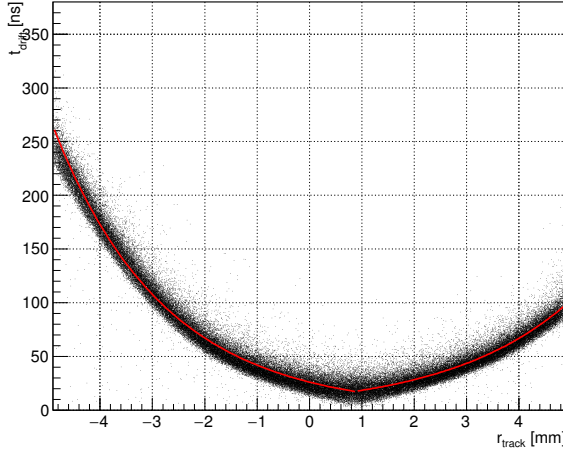


Рис. 16: TR-relation fitting for 0.9mm wire offset value

286 counts as track through the wire:

$$r_{track}(t_{drift} < t_{min}) = r_{wire\ pos} \quad (9)$$

287 where  $t_{min} = \min(t_{drift}(r_{track}))$ ,  $r_{track} = \overline{(-r_{tube}, r_{tube})}$ . Respectively tracks  
 288 with drift time higher than maximum of fit function range artificially counts as  
 289 tracks with near tangents to the tube position  $r_{track} = \pm r_{tube}$  (because efficiency  
 290 decreases near the tube wall down to 20%).

### 291 6.3 Track reconstruction precision

292 Obviously precision is head factor when during we decide design of detector.

293 The STRAW tube tracker should be as light as possible to avoid multiple  
 294 scattering on structural components of detector. But design should be changed  
 295 within reason if precision suffers from this<sup>3</sup>.

296 How precision of track reconstruction depends on wire position(wire di-  
 297 placement)?

298 As you can see on figure ?? there are no significant difference of track  
 299 reconstruction precision between two mode of wire location despite of the increas-  
 300 ing drift time for displaced wire position(with almost factor of two). The highest  
 301 resolution( $\sim 0.1mm$ ) near the tube wall and worst value  $\sim 0.6mm$  is near  
 302 the wire because the clustering effect. Higher gas pressure should resolve this  
 303 problem.

---

<sup>3</sup>Especially design with no sagging works well for experiment NA62 []. But they have more than 2 times shorter straw when tube have insert in the middle of the tube. So sagging becomes negligible in this case.

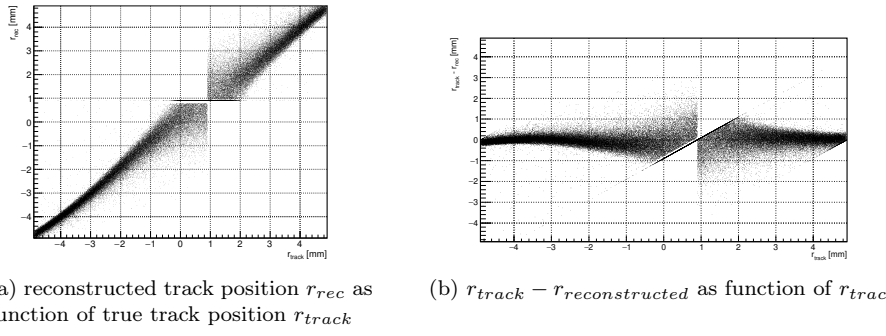


Рис. 17: Distributions of matching of track position to their reconstructed value.

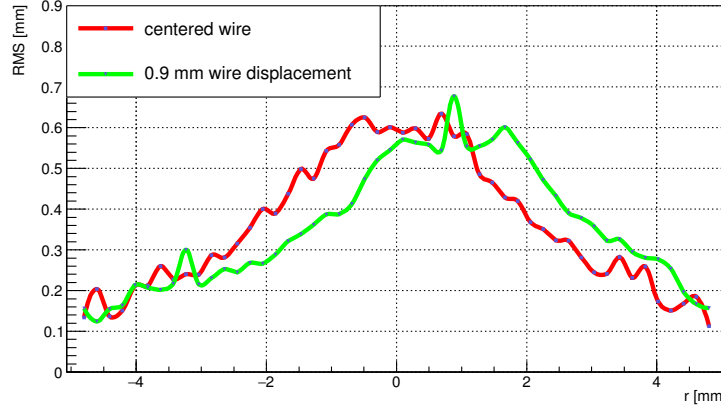


Рис. 18: Comparison of track reconstruction precision for two wire position. Value of precision at every point means RMS of data sample near corresponding track position  $r$ . Red line corresponds to the centered wire position, green line – to the 0.9mm sagged wire position.

## 304 7 Mesurements

305 За період перебування в ЦЕРНі було проведено виміри деяких важливих  
 306 параметрів дрейфової трубки.Хоча довжина тестової трубки сягала порядку  
 307 50 см в довжину, це не завадило провести виміри там де довжина трубки  
 308 не грає ролі.

309 Трубка виготовлена в м. Дубна і поміщена у відповідну механіку яка  
 310 включає в себе кріплення трубки, має канали для циркуляції і газової су-  
 311 міші в трубці, конектори для підведення землі до стінок трубки та високої  
 312 напруги до дроту.

313 Вся система не може похвастатися компактністю, тому уникнути "пара-

зитичних "емностей в місцях де їх не має бути не вдалося. Про міру впливу даного недоліку зараз мова не йде, так як нема з чим порівнювати - конструкція тестового стенду, що включає всі кріплення та фіксації трубки нерозбірна.

Схема підведення, циркуляції і контролю газу в трубці зображена на рисунку 19.

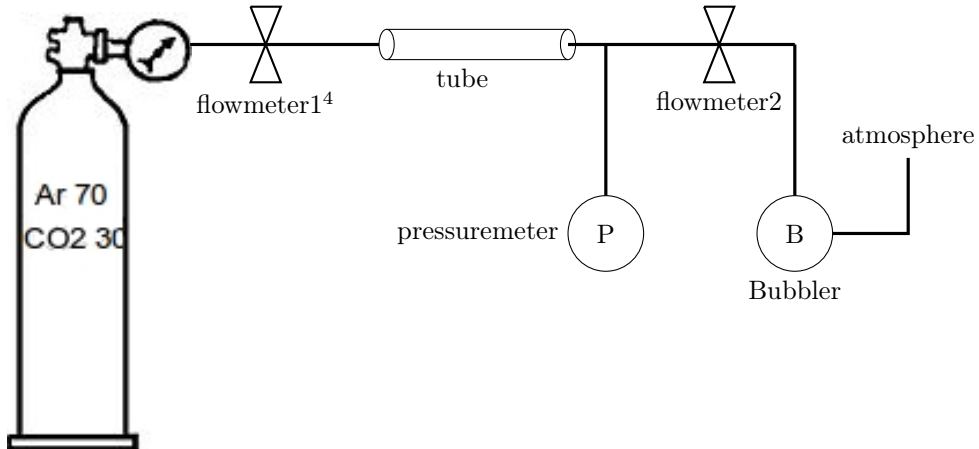


Рис. 19: Gas circulation scheme and circuit of connection of flow control through the drift tube

Електронна схема підключення дрейфової трубки зображена на рис. ??.

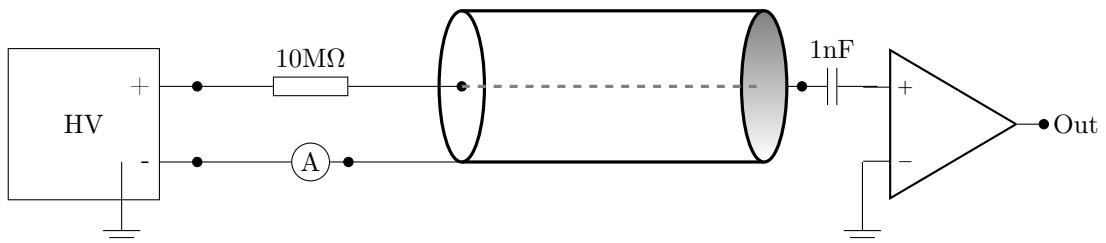


Рис. 20: Електронна схема підключення тестового зразка дрейфової трубки

Ось така досить проста дослідна схема для дослідження зразка трубки.

В нашій наявності було джерело  $Fe^{55}$  яке підходить для калібрування дрейфової трубки.  $Fe^{55}$  в нашому випадку виступає джерелом фотонів з майже моноенергетичним спектром з енергією 5.9 keV.

Першим і найбільш важливим параметром, який необхідно виміряти за допомогою даної установки буде коефіцієнт підсилення сигналу в трубці  $G$  (3).

Ідея полягає в тому, щоб виміряти заряд, що протікає через в електричному колі трубки. Будемо дотримуватися тієї точки зору, що струм через

330 амперметр (see fig. 20) за відсутності радіоактивного  $I_0$  джерела буде ста-  
 331 лий з часом. Цей струм може мати місце в результаті струмів витоку в  
 332 колі або ж фактом реєстрації трубкою фонових частинок(наприклад атмо-  
 333 сферних мюонів). Тож за наявності джерела  $Fe^{55}$  весь надлишковий струм  
 334  $\Delta I = I - I_0$  в колі дрейфової трубки буде пов'язаний лише з реєстрацією  
 335 гамма-квантів джерела  $Fe^{55}$ .

336 З іншої сторони  $\Delta I$  можна виразити через початкову кількість електро-  
 337 нів та коефіцієнт газового підсилення (10):

$$\Delta I = GN_0e; \quad (10)$$

338 тут  $G$  - коефіцієнт газового підсилення;  $N_0$  - кількість початкових електрон-  
 339 іонних пар за одну секунду,  $e$  - заряд електрона в Кл.

340 В свою чергу  $N_0$  можна виразити як.

$$N_0 = R \langle n \rangle = R \sum_n np(n) \approx R \int_0^{\infty} np(n) dn; \quad (11)$$

341 Тут  $p(n)$  - імовірність того, що фотон з енергією 5.9 КеВ провзаємодівши  
 342 з атомом аргону утворить  $n$  електрон іонних пар,  $R$  - частота реєстрації  
 343 сигналів [Hz] так як нам потрібно знайти кількість електрон-іонних пар за  
 344 час 1с.

345 Розрахунок розподілу  $p(n)$  в GARFIELD подано на рисунку 21. Як видно  
 346 з рисунку в розподілі  $p(n)$  присутньо 2 піки: основний фотопік, та менший  
 347 escape peak. Escape peak for argon is known to be 3.2 keV less than the primary  
 348 peak. An escape peak is formed by a number of photon interactions in the gas  
 349 resulting in one primary ionization electron and a re-emitted X-ray with a long  
 350 mean free path.

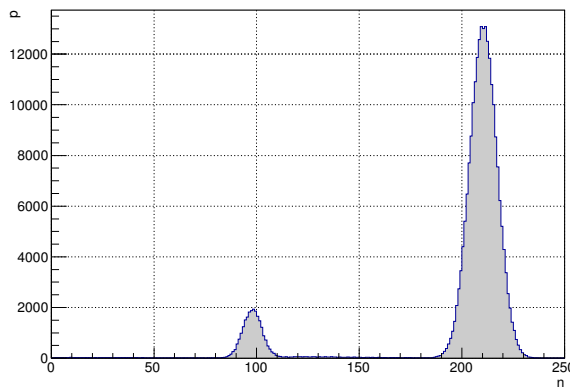


Рис. 21: Розподіл актів взаємодії фотонів енергії 5.9 кеВ з газом Аргону від  
 кількості первинних електронів, утворених в об'ємі дрейфової трубки

351        Все виглядає досить просто. На виході з підсилювача 20 сигнал пода-  
352       ється на дискримінатор з порогом спрацьування виставленим на рівні  
353       достатньому для реєстрації сигналів але достатньо високим, щоб шум не за-  
354       раховувався. Сигнал з дискримінатора у вигляді прямокутного сигналу  
355       подається на лічильних, який спрацьовує по зростаючому фронту. Така  
356       схема має малий мертвий час порядку  $XXX$ , тому для частоти сигналів  
357        $R \sim 5000 \frac{\text{events}}{\text{second}} \approx 200 \frac{\mu\text{s}}{\text{event}}$  кількість незарахованих сигналів буде нищівно  
358       мала.

359        Для першої оцінки коефіцієнту підсилення ми припускаємо про таку собі  
360       суперпозицію лавин і лінійну маштабованість амплітуди кінцевого сигналу  
361       від кількості початкових електронів(далі ми покажемо що це не так).

362        З розподілу на рис.21 знаходимо  $\langle n \rangle = 197.87$  для середньої кількість  
363       первинних електронів від акту взаємодії фотону енергії  $5.9keV$  з атомами  
364       газу  $Ar 70\% + CO_2 30\%$ .

365        Результати вимірювань представимо у вигляді таблиці 2

### 366       **7.1 Поправка на кучність просторового заряду**

367        Тестове джерело  $fe^{55}$  є джерелом гама квантів енергії  $\sim 5.9keV$  які в разі  
368       фотоекскту з атомами газу аргону утворюють  $\sim 200$  іон-електронних пар.  
369        Під дією сильного електричного поля між анодом і катодом така хмара  
370       електронів починає дрейфувати в напрямку дроту. Будь який просторовий  
371       заряд утворює своє власне  $e/m$  поле чим викривлює зовнішнє. В результаті  
372       парціальні лавини на окремій первинний електрон хмари утворюють лавину  
373       мершого розміру порівняно з одиничним електроном(як нприклад від іоні-  
374       зації мюооном).

375        Даний ефект був спостережений на практиці.

376        Кожних сигнал на виході з підсилювача відрізняється за амплітудою в  
377       залежності від кількості первинних електронів що спровокувала його. То  
378       ж цілком справедливо на в експериментальному спектрі сигналів побачити  
379       два горби подібно до розрахованого в GARFIELD спектру  $p(n)$ .

pressure [bar]	Rate [Hz]	Voltage [V]	Current [nA]
1 (0.856 a.o.)	4857	1600	$1.72 \pm 0.22$
=	=	1650	$2.81 \pm 0.13$
=	=	1700	$4.54 \pm 0.23$
=	=	1750	$7.36 \pm 0.33$
=	=	1800	$11.40 \pm 0.55$
=	=	1850	$16.91 \pm 0.85$
=	=	1900	$24.11 \pm 1.05$
1.1 (0.906 a.u.)	5263	1600	$1.00 \pm 0.18$
=	=	1650	$1.62 \pm 0.09$
=	=	1700	$2.60 \pm 0.12$
=	=	1750	$4.12 \pm 0.16$
=	=	1800	$6.54 \pm 0.29$
=	=	1850	$10.13 \pm 0.39$
=	=	1900	$15.02 \pm 0.69$
1.2 (0.951 a.u.)		1600	$0.65 \pm 0.06$
=		1650	$1.04 \pm 0.07$
=		1700	$1.62 \pm 0.08$
=	5409	1750	$2.56 \pm 0.12$
=		1800	$4.05 \pm 0.17$
=		1850	$6.34 \pm 0.25$
=		1900	$9.60 \pm 0.40$
1.3 (0.998 a.u.)		1600	$0.42 \pm 0.04$
=		1650	$0.66 \pm 0.05$
=		1700	$1.02 \pm 0.06$
=	5023	1750	$1.60 \pm 0.13$
=		1800	$2.50 \pm 0.12$
=		1850	$3.89 \pm 0.18$
=		1900	$5.98 \pm 0.24$

Табл. 2: short tube measurements. Threshold equal to 32 mV.

## 380 8 Додаток

### 381 8.1 pressure meter

382 Для вимірювання тиску в дрейфовій трубці використувався датчик ти-  
 383 ску(pressure transmitters) від компанії SensorTechnics®. На приладі зазна-  
 384 чено ідентифікаційний код ID:CTE9005AQ4, по якому було знайдено відпо-  
 385 відну документацію від виробника [4].

Gain(no cor)	P [bar](U[V])	HV [V]	Thr [mV]	I [nA]	RMS [nA]	Rate [Hz]
11138	1.0(0.857)	1600		-1.7700	0.0919	=
18196	1.0(0.857)	1650		-2.8915	0.1598	=
29255	1.0(0.857)	1700	32	-4.6490	0.2328	4965.9
47012	1.0(0.858)	1750		-7.4707	0.4380	=
73159	1.0(0.857)	1800		-11.6257	0.5630	=
9885	1.1(0.906)	1650		-1.6921	0.1099	=
15747	1.1(0.905)	1700		-2.6955	0.13381	=
25275	1.1(0.905)	1750	32	-4.3263	0.1975	5349.0
39887	1.1(0.906)	1800		-6.8274	0.2841	=
61359	1.1(0.906)	1850		-10.5028	0.4567	=
9260	1.2(0.951)	1700		-1.6921	0.1053	=
14536	1.2(0.951)	1750		-2.6562	0.1274	=
22991	1.2(0.951)	1800	32	-4.2012	0.1900	5710
35777	1.2(0.951)	1850		-6.5376	0.2880	=
54684	1.2(0.951)	1900		-9.9924	0.5284	=
5444	1.3(0.998)	1700		-1.03	0.06	=
8351	1.3(0.998)	1750		-1.58	0.14	=
13267	1.3(0.998)	1800		-2.51	0.12	=
20615	1.3(0.998)	1850	32	-3.90	0.15	5987
31716	1.3(0.998)	1900		-6.00	0.29	=
48102	1.3(0.998)	1950		-9.10	0.38	=
69987	1.3(0.998)	2000		-13.24	0.50	=
100751	1.3(0.998)	2050		-19.06	0.78	=

Табл. 3: Table 2

## Література

- <sup>386</sup> [1] <http://garfield.web.cern.ch/garfield>
- <sup>387</sup> [2] thesis Kozlinskiy.pdf
- <sup>388</sup> [3] NA62 Technical Design Report from December 2010.
- <sup>389</sup> [4] DataSheet for Pressure transmitters for corrosive liquids and gases  
CTE/CTU9000 series. [http://www.first-sensor.com/cms/upload/datasheets/DS\\_Standard-CTE-CTU9000\\_E\\_11509.pdf](http://www.first-sensor.com/cms/upload/datasheets/DS_Standard-CTE-CTU9000_E_11509.pdf)
- <sup>390</sup>
- <sup>391</sup>
- <sup>392</sup>